Supplementary Information

Introducing Vacancy Defects to Induce Ferroelectric-like Switching in Antiferroelectric Oxides

Anil Adukkadan*, Pooja Punetha and Rajeev Ranjan
Department of Materials Engineering,
Indian Institute of Science,
Bengaluru, Karnataka, India- 560012

**Corresponding Author- Anil Adukkadan*
Email: anilpakkam@gmail.com

Figure S1 (a) XRD patterns of (i) PNZST53/35/12, PNZST53/38/09, and PNZST53/40/07; patterns in the 2θ range 37-45° is given in (b).

Figure S2 (a) XRD patterns of $Pb_{0.995}(Zr_{0.53}Sn_{0.40}Ti_{0.07})_{0.99(1-x)}Nb_{0.01}Fe_xO_3$; patterns in the 2θ range 37-45° are given in (b).

Figure S3 (a)-(c) P-E, S-E and I-E hysteresis curves of PNZST53/35/12, PNZST53/38/09 and PNZST53/40/07.

Figure S4 (i) P-E hysteresis curves (ii) first and second cycle S-E curves (iii) first and second cycle I-E curves of $Pb_{0.995}(Zr_{0.53}Sn_{0.40}Ti_{0.07})_{0.99(1-x)}Nb_{0.01}Fe_xO_3$; x=(a) 0.012, (b) 0.020, (c) 0.024.

Figure S5 In-situ XRD patterns of $Pb_{0.995}(Zr_{0.53}Sn_{0.40}Ti_{0.07})_{0.99(1-x)}Nb_{0.01}Fe_xO_3$; (a)x=0; (b)0.030 in the 2θ range 37.5- 38.5 °, 43.5- 44.5° and 80.5- 81.5 ° at room temperature by applying an electric field of reverse polarity

Figure S6 XPS spectrum of Fe2p of $Pb_{0.995}(Zr_{0.53}Sn_{0.40}Ti_{0.07})_{0.99(1-x)}Nb_{0.01}Fe_xO_3$ ceramics; (a) x=0.010 and (b) x=0.030.

Figure S7 (a)-(c) P-E, S-E and I-E hysteresis curves of $Pb_{0.995}(Zr_{0.53}Sn_{0.40}Ti_{0.07})_{0.99(1-x)}Nb_{0.01}\square_xO_3$; where x=0.010.

Figure S8 (a) P-E hysteresis curves (b) S-E curves of $Pb_{0.995}(Zr_{0.53}Sn_{0.40}Ti_{0.07})_{0.99(1-x)}Nb_{0.01}Fe_xO_3$; x= 0.030.

Figure S9 Le-Bail fitted x-ray diffraction patterns of (a) x=0, (b)x=0.010, (c)x=0.012 at room temperature. {111} and {200} peaks are shown in insets. For fitting, the P4mm space group is used.

Figure S10 Le-Bail fitted x-ray diffraction patterns of (a) x=0.020, (b)x=0.024, (c)x=0.030 at room temperature. {111} and {200} peaks are shown in insets. For fitting, the P4mm space group is used.

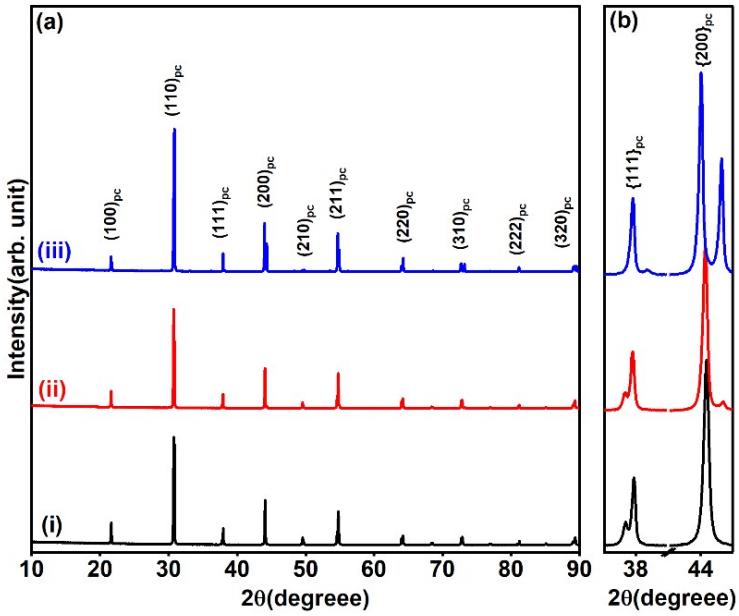

Figure S1 (a) XRD patterns of (i) PNZST53/35/12, PNZST53/38/09, and PNZST53/40/07; patterns in the 2θ range 37-45° is given in (b).

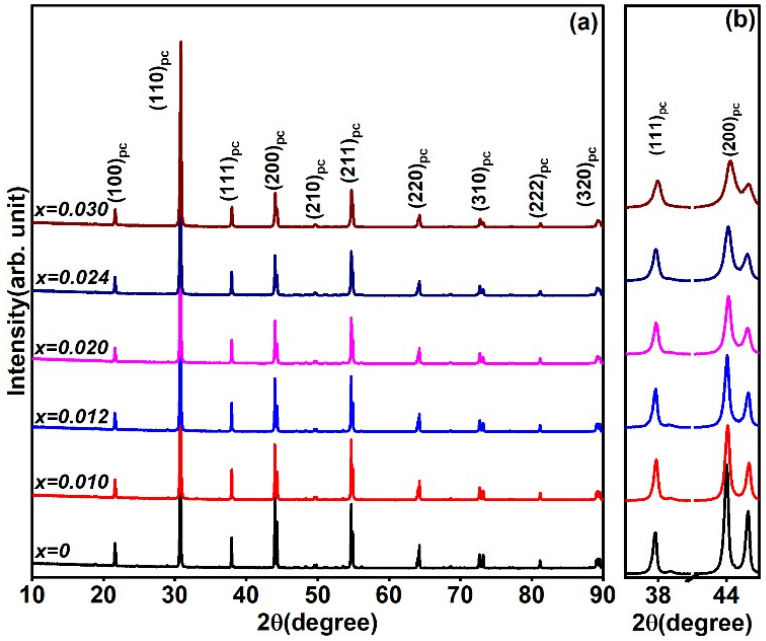

Figure S2 (a) XRD patterns of $Pb_{0.995}(Zr_{0.53}Sn_{0.40}Ti_{0.07})_{0.99(1-x)}Nb_{0.01}Fe_xO_3$; patterns in the 2θ range 37-45° are given in (b).

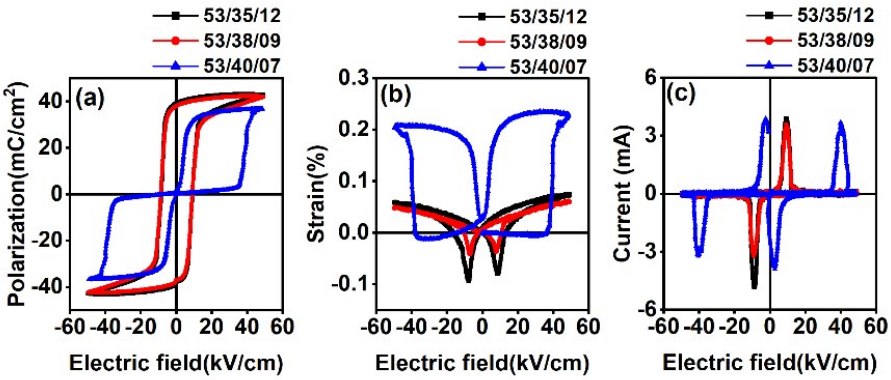

Figure S3 (a)-(c) P-E, S-E and I-E hysteresis curves of PNZST53/35/12, PNZST53/38/09 and PNZST53/40/07.

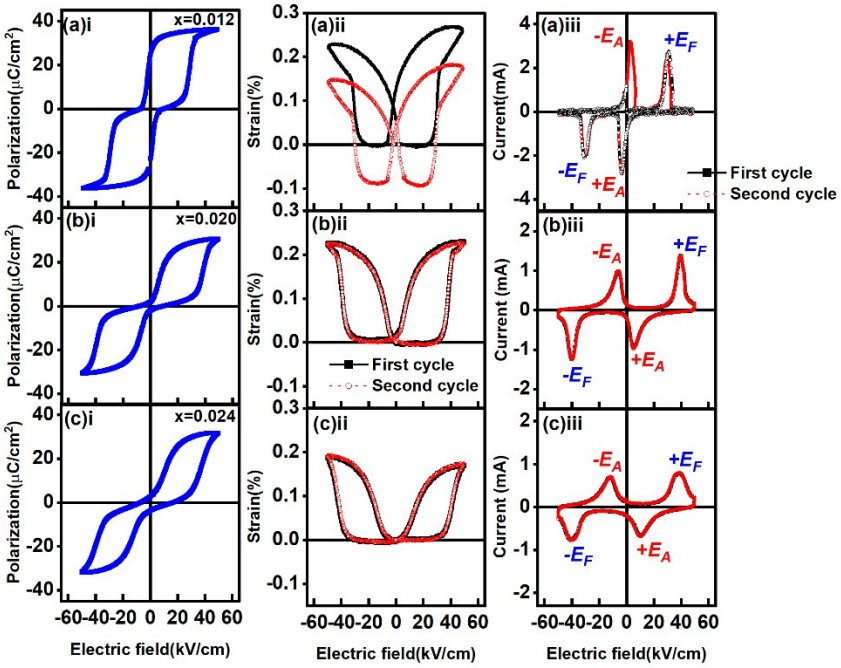

Figure S4 (i) P-E hysteresis curves (ii) first and second cycle S-E curves (iii) first and second cycle I-E curves of $Pb_{0.995}(Zr_{0.53}Sn_{0.40}Ti_{0.07})_{0.99(1-x)}Nb_{0.01}Fe_xO_3$*; x=(a) 0.012, (b) 0.020, (c) 0.024.*

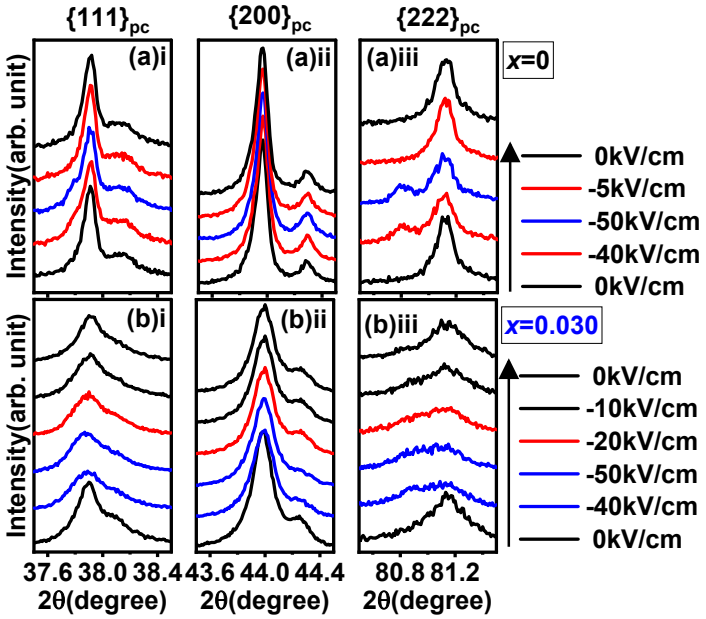

Figure S5 In-situ XRD patterns of $Pb_{0.995}(Zr_{0.53}Sn_{0.40}Ti_{0.07})_{0.99(1-x)}Nb_{0.01}Fe_xO_3$; (a)x=0; (b)x=0.030 in the 2θ range (i) 37.5- 38.5°, (ii)43.5- 44.5° and (iii) 80.5- 81.5° at room temperature by applying an electric field of reverse polarity

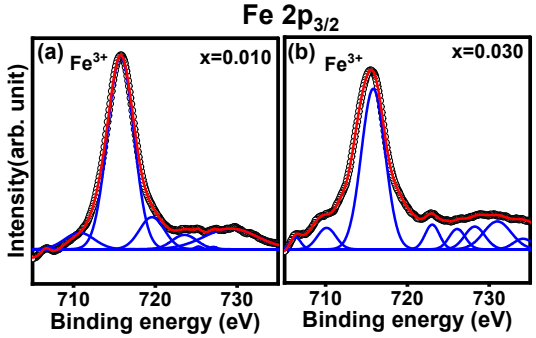

Figure S6 XPS spectrum of Fe2p of $Pb_{0.995}(Zr_{0.53}Sn_{0.40}Ti_{0.07})_{0.99(1-x)}Nb_{0.01}Fe_xO_3$ ceramics; (a) x=0.010 and (b) x=0.030.

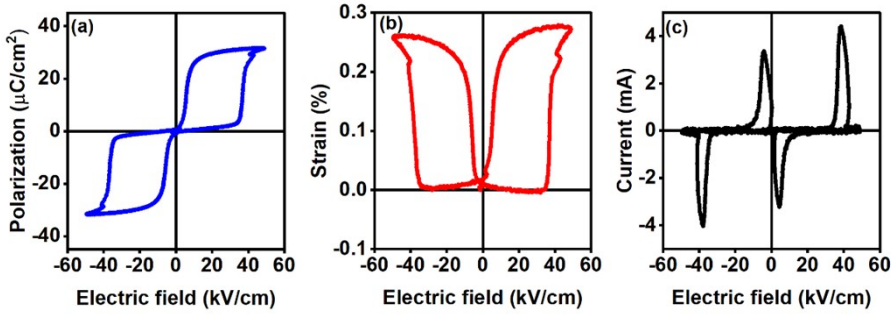

Figure S7 (a)-(c) P-E, S-E and I-E hysteresis curves of $Pb_{0.995}(Zr_{0.53}Sn_{0.40}Ti_{0.07})_{0.99(1-x)}Nb_{0.01}\square_xO_3$; where x=0.010.

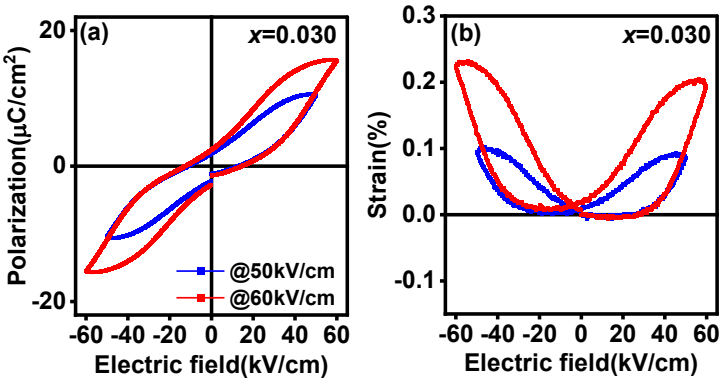

Figure S8(a) P-E hysteresis curves (b) S-E curves of $Pb_{0.995}(Zr_{0.53}Sn_{0.40}Ti_{0.07})_{0.99(1-x)}Nb_{0.01}Fe_xO_3$; x= 0.030.

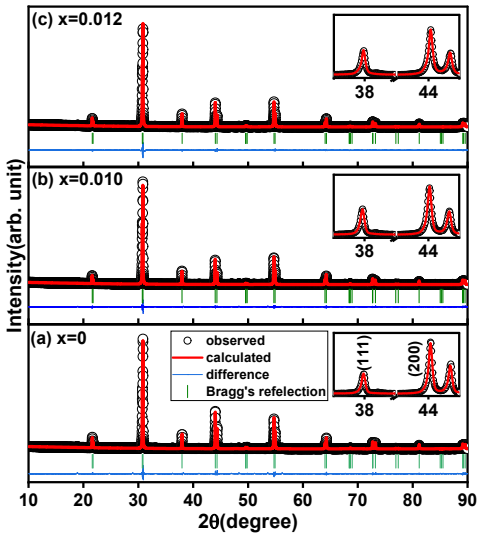

Figure S9 Le-Bail fitted x-ray diffraction patterns of (a) x=0, (b)x=0.010, (c)x=0.012 at room temperature. {111} and {200} peaks are shown in insets. For fitting, the P4mm space group is used.

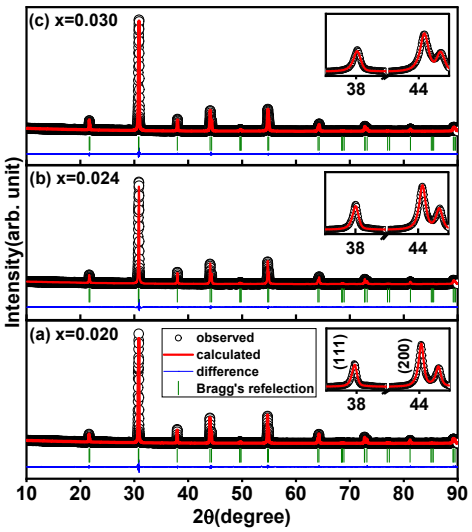

Figure S10 Le-Bail fitted x-ray diffraction patterns of (a) x=0.020, (b)x=0.024, (c)x=0.030 at room temperature. {111} and {200} peaks are shown in insets. For fitting, the P4mm space group is used.